Let it Rain and Snow: Two+ Years of NASA's Global Precipitation Measurement (GPM) Mission Data

*Gail Skofronick Jackson[1]

1.NASA Goddard Space Flight Center

Water is fundamental to life on Earth. Knowing where and how much rain and snow fall globally is vital to understanding how weather and climate impact our Earth's water and energy cycles. The Global Precipitation Measurement (GPM) Core Observatory spacecraft, a partnership with the Japanese, launched February 28, 2014. The GPM instruments are designed to extend the capabilities of the Tropical Rainfall Measuring Mission (TRMM, 1997-2015) by providing global and regional three-dimensional measurements of precipitation for scientific investigations and societal benefit. The cornerstone, or anchor, of the GPM mission is the GPM Core Observatory in a unique 65^{o} non-Sun-synchronous orbit at an altitude of 407 km serving as a physics observatory and a calibration reference to improve precipitation measurements by a constellation of 8 or more dedicated and operational, U.S., Japanese and international passive microwave sensors. The non-sun-synchronous orbit allows for highly sophisticated observations of precipitation in the mid-latitudes where a majority of the population lives. GPM's requirements are to measure rain rates from 0.2 to 110 mm/hr and to detect and estimate falling snow. GPM expands the Tropical Rainfall Measuring Mission (TRMM)'s reach in terms of Earth coverage, inter-calibration of constellation member datasets, coordinated formal-partnership merged precipitation data sets, reduced latency for delivering data products, sophisticated satellite instrumentation, simplified data access, expanded global ground validation efforts and integrated user applications.
GPM is an international satellite mission to unify and advance precipitation measurements from a constellation of partner satellite sensors to provide next-generation precipitation products everywhere every 3 hours (or less). As a science mission with integrated application goals, GPM will also help to monitor water resources, improve forecasting of extreme weather events that lead to floods, droughts, and landslides.
Since launch, GPM has provided unprecedented views of typhoons, extratropical systems, light rain, snowstorms and extreme precipitation. This NASA presentation will include new imagery and scientific insights resulting from the more than two years of GPM data, an overview of the mission concept and science activities, updates on algorithm status, data products and performance, together with information on international collaborations for radiometer inter-calibration and ground validation.

Keywords: Earth, Precipitation, satellite

Precipitation characteristics observed with GPM DPR, in comparison with TRMM PR

*Yukari Takayabu[1], Atsushi Hamada[1], Chie Yokoyama[1], Marika Ono[1]

1.Atmosphere and Ocean Research Institute, the University of Tokyo

Improvements in precipitation measurements with the Dual-frequency Precipitation Radar (DPR) on board the Global Precipitation Measurement (GPM) core satellite, compared to the TRMM/PR are three folds: Extension of the observational region from 36N-36S to 65N-65S, an addition of high-sensitivity Ka-band radar to make the dual frequency measurements available, an improvement of the sensitivity of Ku-band radar itself. In this study, observed characteristics of precipitation by the GPM DPR measurements with those by the TRMM PR measurements are compared in various ways. Rainfall events are defined with contiguous rainfall areas observed with the GPM DPR for March 2014 to December 2015. Size and intensity characteristics of rainfall events in the tropical region (30N-30S) and the mid-latitude regions (30N-65N and 30S-65S) are compared. Area-weighted size histogram comparisons reveal that rainfall events over the tropical oceans have two peaks at meso-alpha and at meso-beta scales, while large meso-alpha size dominates over the mid-latitude oceans. Over land, largest frequency is found in the meso-beta size bin in the tropics, while smaller size bins exhibit more frequency in the mid-latitudes. Maximum precipitation intensity histograms normalized for each 4 categories by event size exhibit larger frequency for heaviest precipitation tails for larger size categories in all N-midlat, N-tropics, S-tropics and S-midlat regions, but dependency on event size is larger in the tropics and more frequent heavy precipitation is found with the largest category in the tropics.
Impacts of the radar sensitivity increase are examined (Hamada and Takayabu, 2016), by comparing Ku-band measurements of with two sensitivity thresholds of corrected reflectivity factors; 12 dBZ and 18 dBZ, representing DPR and PR sensitivity, respectively. Increase of sensitivity results in ~21% in frequency and ~2% in rainfall amount between 40N and 40S. It is shown that, in addition, there is a scientifically significant impact by detecting light anvil precipitation in the upper troposphere with increasing sensitivity with the GPM/DPR observations.

Keywords: Satellite Precipitation Measurements, GPM DPR, Precipitation Characteristics

Improvements in Detection of Light Precipitation with the Global Precipitation Measurement Dual-Frequency Precipitation Radar (GPM/DPR)

*Atsushi Hamada[1], Yukari N Takayabu[1]

1.Atmosphere and Ocean Research Institute, The University of Tokyo

We demonstrates the impact of the enhancement in detectability by the dual-frequency precipitation radar (DPR) on board the Global Precipitation Measurement (GPM) core observatory. By setting two minimum detectable reflectivities--12 and 18 dBZ--artificially to 6 months of GPM DPR measurements, the precipitation occurrence and volume increase by ~21.1% and ~1.9%, respectively, between 40S and 40N.
GPM DPR is found to be able to detect light precipitation, which mainly consists of two distinct types. One type is shallow precipitation, which is most significant for convective precipitation over eastern parts of subtropical oceans, where deep convection is typically suppressed. The other type is probably associated with lower parts of anvil clouds associated with organized precipitation systems.
While these echoes have lower reflectivities than the official value of the minimum detectable reflectivity, they are found to mostly consist of true precipitation signals, suggesting that the official value may be too conservative for some sort of meteorological analyses. These results are expected to further the understanding of both global energy and water budgets and the diabatic heating distribution.
These results are almost based on Hamada and Takayabu (2016, J. Atmos. Oceanic Technol.), but we will also report the results for other seasons, and results used the next version product (V04), which is scheduled to be released within several months.

Keywords: precipitation, satellite, Global Precipitation Measurement (GPM)

Current status of the Global Precipitation Measurement (GPM) mission in Japan

*Riko Oki[1], Takuji Kubota[1], Takeshi Masaki[1], Yuki Kaneko[1], Kinji Furukawa[1], Misako Kachi[1], Yukari Takayabu[2], Toshio Iguchi[3], Kenji Nakamura[4]

1.Japan Aerospace Exploration Agency, 2.University of Tokyo, 3.NICT, 4.Dokkyo University

The Global Precipitation Measurement (GPM) mission is an international collaboration to achieve highly accurate and highly frequent global precipitation observations. The GPM mission consists of the GPM Core Observatory jointly developed by U.S. and Japan and Constellation Satellites that carry microwave radiometers and provided by the GPM partner agencies. The GPM Core Observatory was successfully launched at 3:37 a.m. on February 28, 2014 (JST). The Dual-frequency Precipitation Radar (DPR) was developed by the Japan Aerospace Exploration Agency (JAXA) and the National Institute of Information and Communications Technology (NICT), and installed on the GPM Core Observatory. The GPM Core Observatory chooses a non-sun-synchronous orbit to carry on diurnal cycle observations of rainfall from the Tropical Rainfall Measuring Mission (TRMM) satellite, while the Constellation Satellites, including JAXA's Global Change Observation Mission (GCOM) - Water (GCOM-W) or "SHIZUKU," are launched by each partner agency sometime around 2014 and contribute to expand observation coverage and increase observation frequency. JAXA develops the DPR Level 1 algorithm, and the NASA-JAXA Joint Algorithm Team develops the DPR Level 2 and DPR-GMI combined Level2 algorithms.

JAXA also develops the Global Rainfall Map (GPM-GSMaP) algorithm, which is a latest version of the Global Satellite Mapping of Precipitation (GSMaP), as national product to distribute hourly and 0.1-degree horizontal resolution rainfall map. The GSMaP near-real-time version (GSMaP_NRT) product is available 4-hour after observation through the "JAXA Global Rainfall Watch" web site (http://sharaku.eorc.jaxa.jp/GSMaP) since 2008. To assure near-real-time data availability, the GSMaP_NRT system simplified part of the algorithm and its processing procedure. Therefore, the GSMaP_NRT product gives higher priority to data latency than accuracy, and has been used by various users for various purposes, such as rainfall monitoring, flood alert and warning, drought monitoring, crop yield forecast, and agricultural insurance. There are, however, several requirements from users for GSMaP improvements not only for accuracy but also specification. Among those requests for data specification, the most popular ones are shortening of data latency time and higher horizontal resolution. To reduce data latency, JAXA has developed the GSMaP realtime version (GSMaP_NOW) product for observation area of the geostationary satellite Himawari-8 operated by the Japan Meteorological Agency (JMA). GSMaP_NOW product uses satellite data that is available within 0.5-hour, including GMI, AMSR2 direct receiving data, AMSU direct receiving data and Himawari-8, to produce GSMaP at 0.5-hr before. Then, we are applying 0.5-hour forward extrapolation for future direction by cloud motion vector to produce GSMaP at current hour (GSMaP_NOW) over Himawari-8 observed area. GSMaP_NOW product was released to public in November 2, 2015 through the "JAXA Realtime Rainfall Watch" web site (http://sharaku.eorc.jaxa.jp/GSMaP_NOW/).

Moreover, ground validation (GV) activity using a dual Ka-band radar system developed by JAXA has been conducted along the slope of Mt. Zao in Yamagata, Japan from Oct. 2013 to May 2015. During Dec. 2015-Jan. 2016, the single Ka-radar observation was operated on R/V Mirai of the Japan Agency for Marine-Earth Science and Technology (JAMSTEC) over the Indian Ocean aiming at Maritime precipitation.

After the early calibration and validation of the products and evaluation that all products achieved the release criteria, all GPM standard products and the GPM-GSMaP product has been released to the public since September 2014. The GPM products can be downloaded via the internet

through the JAXA G-Portal (https://www.gportal.jaxa.jp). All GPM standard products will be reprocessing using the updated algorithms (Version 4) on March-April 2016, and the GPM-GSMaP product will be on July 2016.

Keywords: GPM, DPR, GSMaP, ground validation

Quasi-realtime version of the Global Satellite Mapping of Precipitation (GSMaP_NOW) over the Himawari-8 region

*Takuji Kubota[1], Misako Kachi[1], Riko Oki[1]

1.Earth Observation Research Center,Japan Aerospace Exploration Agency

Japan Aerospace Exploration Agency (JAXA) started to distribute the “quasi-realtime” version of the Global Satellite Mapping of Precipitation (GSMaP_NOW) over the Japan Meteorological Agency (JMA) geostationary satellite “Himawari-8” region through the “JAXA Realtime Rainfall Watch” website (http://sharaku.eorc.jaxa.jp/GSMaP_NOW/) since Nov. 2015.
“Realtime availability” of satellite rainfall data is one of major requirements from users. As one of the Japanese products of the the Global Precipitation Measurement (GPM) mission, JAXA has provided the “near-real-time” GSMaP (GSMaP_NRT) product, which is hourly and 0.1-degree grid box global rainfall product combining observation data from microwave and infrared radiometers aboard multiple satellites, four hours after observation through the “JAXA Global Rainfall Watch” website (http://sharaku.eorc.jaxa.jp/GSMaP/). Data latency of “four hours” for GSMaP_NRT product was chosen considering balance of satellite data availability and user requirements. To produce GSMaP_NRT, we allocated three hours to collect satellite data and one hour to process data. Users and purposes of GSMaP_NRT data have been increased in number and variety since its release. It is used in, for example, rainfall monitoring, flood alert and warning, drought monitoring, crop yield forecast, and agricultural insurance.
Building on its experience in the GSMaP production, JAXA has developed the GSMaP realtime version (GSMaP_NOW) product to respond user requirements to shorten data latency of “four hour,” and achieved this by providing current rainfall over the geostationary satellite Himawari-8 region. The GSMaP_NOW product uses passive microwave radiometer and geostationary satellite data that is available only within 0.5-hour after observation. At present, we uses data from GPM/GMI, GCOM-W/AMSR2 direct broadcasting near Japan, NOAA and MetOp’s AMSU/MHS direct broadcasting, and Himawari-8/AHI to produce GSMaP at 0.5-hour before. In addition, extrapolation of rainfall area with 0.5-hour forward (toward future) by using cloud moving vector calculated from AHI enables us to produce “quasi-realtime” rainfall map over Asian regions. All processing are completed within 0.5-hour, and updated half-hourly.
GSMaP_NOW and other GSMaP products are validated by comparing with with JMA’s gauge-calibrated radar analysis (Radar-AMeDAS) over the Japan in daily and 0.25-degree grid basis. Results showed that accuracy of GSMaP_NOW is almost equivalent or slightly worse than GSMaP_NRT for the period from October 2015 to December 2015.
This quasi-realtime capability will provide possibility to operational users to apply the GSMaP_NOW data in their rainfall monitoring more rapidly, flood alert in smaller basins. Extension of GSMaP_NOW from “Himawari” area to the other geostationary satellites’ observation areas is also under consideration for future improvements.

Keywords: GPM, GSMaP, Realtime

Future precipitation measuring mission from space

*Nobuhiro Takahashi[1], Kinji Furukawa[2], Misako Kachi[2], Yusuke Muraki[2], Riko Oki[2]

1.Institute for Space-Earth Environmental Research, Nagoya University, 2.JAXA

Since the launch of Global Precipitation Measurement (GPM)/Core satellite in February 2014, the dual frequency precipitation radar (DPR) that is the key instrument of GPM has been working nominally with better performance than expected. The success of the GPM/DPR demonstrates the feasibility of the precipitation radar technology is now well established with high reliability. It also leads the expectation of use of the radar for more general purpose of precipitation like passive microwave radiometers and for more next step of the precipitation study. In this paper, current direction of the future precipitation-measuring mission is reported as well as the possible mission plans. In addition, since the nominal lifetime of the GPM/Core satellite is 5 years, we need to prepare the future precipitation-measuring mission now.

Two types of the directions are considered as the follow-on mission of the GPM/core: 1) development of the smaller and cheap radar satellite by using the GPM/DPR technology and the current advanced radar technologies such as power device (e.g. GaN) and the pulse compression technique to gain the sensitivity significantly, and 2) development of the DPR type radar with better sensitivity and the wider swath observation. The former has advantages on the cost that leads the multiple radar satellite observation and also leads the great improvement of the hourly global precipitation map (such as GSMaP) because of the utilization of the radar data directly into the precipitation map. The low cost satellite can be purchased by other countries. Considering that the satellite altitude is 800 km with inclination angle of less than 30 degrees and the radar aperture is quarter of the KuPR (Ku-band radar with 2.2 x 2.2 m aperture) on GPM/Core, the sensitivity is about 20 dBZ for each resolution of about 20 km and the swath width is about 800 km that corresponds to the 3 to 6 hourly observation between 30 degree south and the 30 degree north. The latter is more scientific purpose such as cloud-precipitation processes relating to the assessment of the impact to the precipitation by the climate change such as global warming. The response of the precipitation systems to the climate change is one of the most unknown and the most concerned parameter of the global warming issue. Both the numerical simulation studies and observational study are essential to reveal this issue and the satellite observation is the only the tool to cover the global precipitation with equal quality. Since current issues of the precipitation radar are the sensitivity and the swath width (also sampling frequency), improvement of the DPR is essential. The sensitivity can be improved by introduce the current power device and pulse compression system and the swath width can be extended even current DPR design based on the special experiment during the end of mission of the TRMM satellite. The goal of the sensitivities of both KuPR and KaPR are -10 dBZ with twice wider swath width of GPM/KuPR (490 km). Sensitivity budget with current technology indicates that the achievable sensitivity is about 0 dBZ; even this number is great improvement from GPM/DPR.

The future goal of the radar technology is observation from the geostationary orbit; the merits are the continuous observation with Doppler velocity measurement and the demerits are the sensitivity (> 20 dBZ) and horizontal resolution (20 km) assuming the 30 m diameter antenna. Continuous observation makes it possible to monitor the precipitation system such as typhoons and to directly utilize the numerical weather prediction. Current technology indicates that the radar observation from the geostationary orbit is possible with current radar technology if you can develop the 30 m diameter antenna.

Keywords: Precipitation Measurement, Satellite

Development status of the GCOM-W1 AMSR2 research products

*Takashi Maeda[1], Mieko Seki[2], Tomoyuki Nomaki[2], Misako Kachi[1]

1.Japan Aerospace Exploration Agency, 2.Remote Sensing Technology Center of Japan

Japan Aerospace Exploration Agency (JAXA) has operated the Advanced Microwave Scanning Radiometer 2 (AMSR2) onboard the GCOM-W satellite lauched in May 2012. In this mission, 8 geophysical values (water
vapor, cloud liquid water, precipitation, sea surface temperature, sea surface wind speed, sea ice concentration, snow depth, and soil moisture) were defined as the standard products, and these are released to the public since May 2013.
On the other hand, several research products (e.g., land surface temperature, vegetation water content, sea
ice motion vector, thin sea ice detection, and high-resolution sea ice concentration) as a candidate of a future
standard product were officially defined in March 2015. Based on it, we started to implement algorithms to create the research products from the AMSR2 data, and obtained the initial validation results. In this paper, we present the current status of GCOM-W AMSR2 research products.

Keywords: Watercycle monitoring, Microwave radiometer, Earth observation

Impact of all-sky microwave radiance assimilation on typhoon forecasts in JMA global NWP system

*Masahiro Kazumori[1]

1.Japan Meteorological Agency

Space-based microwave radiance observations provide essential information for today’s numerical weather prediction (NWP). The data contain information on atmospheric water vapor, cloud and precipitation under clear and cloudy conditions. In order to use the information, an all-sky microwave radiance assimilation method for the JMA global data assimilation system has been developed. In the all-sky assimilation, several microwave imagers’ radiance data (e.g. AMSR2/GCOM-W, GMI/GPM and SSMIS/DMSP) were evaluated and their first guess (FG) departures (observed radiance minus simulated radiance) were examined. The all-sky FG departure statistics revealed biases originated from cloud physics scheme of the JMA global model. Results of assimilation experiments indicate that there are excessive light rain areas forecasted in the tropics and cloud liquid water amounts are underestimated in stratocumulus areas. These biases in the FG departure are issues in the all-sky radiance assimilation at JMA. Furthermore, the assimilation showed an undesirable impact as a decrease of analyzed mean water vapor amount. However, in spite of these issues, preliminary experiment of the all-sky microwave radiance assimilation showed positive impacts on tropical cyclone track prediction, intensity prediction and made better FG fit to wind and humidity observations. In the tropical cyclone cases, analyzed water vapor fields and forecasted precipitation features became much realistic than those of in clear sky assimilation. Comparisons of the all-sky radiance assimilation and the clear-sky assimilation for several typhoon cases are presented in the conference.

Keywords: Numerical Weather Prediction, microwave radiance, data assimilation

Satellite data assimilation using NICAM-LETKF

*Koji Terasaki[1], Shunji Kotsuki[1], Takemasa Miyoshi[1]

1.RIKEN Advanced Institute for Computational Science

Data assimilation plays an important role in increasing the accuracy of the numerical weather prediction (NWP). We applied the Local Ensemble Transformed Kalman Filter (LETKF) to the atmospheric general circulation model NICAM (Non-hydrostatic ICosahedral Atmospheric Model). In this study, the conventional observations, satellite microwave radiances from AMSU-A (Advanced Microwave Sounding Unit-A), and satellite-based global precipitation data GSMaP (Global Satellite Mapping of Precipitation) are assimilated. It is difficult to assimilate precipitation observations because of the non-Gaussian error distribution and highly nonlinear precipitation process. Methods are developed to get benefits from these three types of observations. The results indicate that adding more observations makes the analysis more accurate.

Keywords: data assimilation, AMSU-A, GSMaP

On the Algorithm to Discriminate Cloud and Precipitation Particle Type from CloudSat and CALIPSO

*Maki Kikuchi[1], Hajime Okamoto[2], Kaori Sato[2], Yuichiro Hagihara[1]

1.Japan Aerospace Exploration Agency/Earth Observation Research Center, 2.Kyushu University/Research Institute for Applied Mechanics

Cloud and precipitation take key role in the climate system. Information on the cloud phase, shape, rain and snow (hereafter, hydrometeor particle type) are important factors that determine the radiative properties of cloud and precipitation. The knowledge of the hydrometeor type is also necessary to retrieve their microphysical properties, such as liquid/ice/rain/snow water content and effective radius. In this study, we first derived the hydrometeor particle type for a cloud profiling radar (CPR) onboard CloudSat and Mie-scattering lidar, Cloud-Aerosol Lidar with Orthogonal Polarization (CALIOP), onboard Cloud-Aerosol Lidar and Infrared Pathfinder Satellite Observation (CALIPSO), independently. The CloudSat and CALIPO are in operation since June 2006 and they have accumulated vertical profiles of cloud and precipitation over the globe for ten years. The final synergy hydrometeor particle type was derived by comparing the discrimination results from CloudSat and CALIPSO and registering a type that was most reasonable. The CALIOP algorithm was based on the previous scheme originally developed by Yoshida et al. [2010] and modified by Hirakata et al. [2014]. The CPR algorithm consisted of three main steps: (1) initial type classification by radar reflectivity and European Center for Medium-range Weather Forecasting (ECMWF) temperature; (2) precipitation correction by attenuation corrected surface radar reflectivity; and (3) spatial continuity test. The initial type classification was conducted by selecting a type from a look-up-table of CPR radar reflectivity and ECMWF temperature. The look-up-table was constructed using the cloud particle type discrimination from CALIOP and the precipitation detection by Precipitation Radar (PR) onboard Tropical Rainfall Measuring Mission (TRMM). For each CloudSat bin, an initial type was selected from the look-up-table that corresponded to the observed radar reflectivity and ECMWF temperature. The second step was the precipitation correction. Each profile was determined whether it was a precipitating profile or not by a simple threshold method of attenuation corrected surface radar reflectivity (Haynes et al. [2009]). If the profile was detected as precipitation but the initial classification had been registered as a cloud profile, the initial classification of the lowest hydrometeor classification was corrected to precipitation (and visa-versa). The last step of the CPR algorithm was the spatial continuity test to eliminate spike misclassification. The final CPR-CALIOP synergy scheme classified the hydrometer particles into 7 types: warm water, supercooled water, randomly oriented ice crystals (3D-ice), horizontally oriented plates (2D-plate), mixture of 3D-ice and 2D-plate, rain and snow. Taking the advantage of CPR's capability to penetrate cloud and light precipitation and CALIOP's capability to detect thin clouds, the synergy algorithm derived the global vertically resolved distribution of hydrometeor particle types from thin cirrus clouds to light precipitation.
The hydrometeor particle type algorithm is considered to be applied in upcoming Earth Clouds, Aerosols and Radiation Explorer (EarthCARE) Level 2 Standard Products that will be processed and released from JAXA to observe global and vertical distribution of the hydrometeor particle types.

Keywords: cloud radar, lidar, satellite, cloud observation, precipitation observation

Synergistic use of multisensor satellite observations for quantification of cloud processes and climate model diagnostics

*Suzuki Kentaroh[1]

1.Atmosphere and Ocean Research Institute, University of Tokyo

It is now recognized that key questions in climate sciences cannot be addressed with a single satellite observation alone. This recognition is an underlying motivation for emerging/existing multisensor satellite observations. One particular area of research to be advanced with such multisensor satellite observations is a characterization of physical processes in climate system, which still is a fundamental uncertainty in climate modeling. Cloud processes, among others, are one of the most uncertain components in state-of-the-art climate models and therefore are a particular target of studies that should be conducted with a synergistic use of multisensor satellite observations. In this presentation, I highlight our recent progress in combining multiple NASA satellites to obtain novel insight into cloud processes, which also has enabled a new “process-oriented” type of climate model diagnostics. In particular, we have developed methodologies for combining simultaneous measurements of cloud and precipitation provided by CloudSat and Aqua/MODIS. The methodologies exploit the unique measurement capability of the two sensors to construct the particular statistics that “fingerprint” the particle growth processes in warm clouds. Our recent investigation for land-ocean differences found in the statistics is also discussed in this presentation to identify a key role of updraft velocity in the warm rain formation. This points to a necessity for measuring updraft velocity from space in our future satellite mission. The observation-based statistics also serve as a reference for evaluating climate models in their representations of fundamental cloud processes. The methodologies developed have indeed been applied to a hierarchy of models, including global climate models and global/regional cloud-resolving models, to identify their key biases in representations of fundamental microphysical processes. Such a new process-based model constraint has also been contrasted against a traditional “performance-oriented” model evaluation based on historical trends of global mean temperature to expose their apparent dichotomy. This implies the presence of compensating errors at a fundamental process level in current climate models and underscores the necessity of further efforts for “process-oriented” model diagnostics with a synergistic use of upcoming multiple satellite observations.

Vertical profile of cloud and radiation budget observed by satellite

*Tadahiro Hayasaka[1], Ayano Mitsui[1], Naoya Takahashi[1]

1.Graduate School of Science, Tohoku University

Vertical profile of cloud is obtained from space-borne active sensors such as CPR/CloudSat and CALIOP/CALIPSO. We used three CloudSat products, 2B-GEOPROF-LIDAR, 2B-TAU, and 2B-FLXHR-LIDAR to reveal spatial and seasonal properties of clouds. Cloud vertical profiles are classified into 10 types referred to ISCCP. Obtained cloud profiles are discussed with meteorological and sea surface conditions such as wind, water vapor surface air temperature and sea surface temperature. The results show that a combination of low-cloud and high-cloud is frequently observed in tropical and mid-latitude regions and these clouds are formed according to different mechanisms. It is also shown that overlapping of cloud affect longwave radiation budget at the top of the atmosphere. Overlying cloud decreases the cooling rate at the uppermost layer of low-cloud, and it affect the formation and dissipation of low-cloud. In the analysis of three data products, some inconsistency was found, which was attributed to unsuccessful retrieval of cloud water content and effective radius of cloud particle. Therefore, it is noted that quantitative evaluation of the product is critical to application of these cloud data to radiation and climate change studies.

Keywords: cloud, radiation, satellite

Global Distribution of Vertical Wavenumber Spectra in The Lower Stratosphere Observed Using High-Vertical-Resolution Temperature Profiles from COSMIC GPS Radio Occultation

*Noersomadi Noersomadi[1], Toshitaka Tsuda[2]

1.Graduate Student of Graduate School of Science, Kyoto University, 2.Research Institute for Sustainable Humanosphere (RISH), Kyoto University

We retrieved temperature (*T*) profiles with a high vertical resolution using the full spectrum inversion (FSI) method from the Constellation Observing System for Meteorology, Ionosphere and Climate (COSMIC) GPS radio occultation (GPS-RO) data from January 2007 to December 2009. We studied the characteristics of temperature perturbations in the stratosphere at 20–27 km altitude. This height range does not include a sharp jump in the background Brunt–Vaisala frequency squared (N^2) near the tropopause, and it was reasonably stable regardless of season and latitude. We analyzed the vertical wavenumber spectra of gravity waves (GWs) with vertical wavelengths ranging from 0.5 to 3.5 km, and we integrated the (total) potential energy E_p^T. Another integration of the spectra from 0.5 to 1.75 km was defined as E_p^S for short vertical wavelength GWs, which was not studied with the conventional geometrical optics (GO) retrievals. We also estimated the logarithmic spectral slope (p) for the saturated portion of spectra with a linear regression fitting from 0.5 to 1.75 km.
Latitude and time variations in the spectral parameters were investigated in two longitudinal regions: (a) 90–150° E, where the topography was more complicated, and (b) 170–230° E, which is dominated by oceans. We compared E_p^T, E_p^S, and p, with the mean zonal winds (U) and outgoing longwave radiation (OLR). We also show a ratio of E_p^S to E_p^T and discuss the generation source of E_p^S. E_p^T and p clearly showed an annual cycle, with their maximum values in winter at 30–50° N in region (a), and 50–70° N in region (b), which was related to the topography. At 30–50° N in region (b), E_p^T and p exhibited some irregular variations in addition to an annual cycle. In the Southern Hemisphere, we also found an annual oscillation in E_p^T and p, but it showed a time lag of about 2 months relative to U. Characteristics of E_p^T and p in the tropical region seem to be related to convective activity. The ratio of E_p^T to the theoretical model value, assuming saturated GWs, became larger in the equatorial region and over mountainous regions.

Overview and status of the JAXA Himawari Monitor

*Misako Kachi[1], Maki Kikuchi[1], Yukio Kurihara[1], Takashi Nagao[1], Hiroshi Murakami[1]

1.Earth Observation Research Center, Japan Aerospace Exploration Agency

In October 2014, new geostationary meteorological satellite “Himawari-8” operated by the Japan Meteorological Agency (JMA) was launched from the JAXA Tanegashima Space Center. Himawari-8 has started its operation at 02 UTC on 7 July 2015, replacing the geostationary meteorological satellite “MTSAT-2”.Since there are many commonalities and synergies between the Himawari-8 and JAXA’s upcoming Earth observation satellites, such as the Global Change Observation Mission –Climate (GCOM-C) to be launched in Japanese Fiscal Year (JFY) of 2016, Greenhouse gasses Observing SATellite-2 (GOSAT-2), and EarthCARE mission to be launched in JFY2017, JAXA cooperates with JMA in algorithm development, calibration and validation activities on the Himawari-8 satellite. JAXA also exchanged agreements with JMA to promote the Himawari-8 data in research and education community. To this purpose, we received the Himawari data from JMA in near-real-time basis, and distribute its images and data through the JAXA Himawari Monitor (http://www.eorc.jaxa.jp/ptree/). We developed algorithms, which will be consistent with those for the GCOM-C, GOSAT-2 and EarthCARE missions, to retrieve geophysical parameters from the Himawari-8 data with collaboration of external institutions. As of February 2016, aerosol properties and sea surface temperature (SST) products are provided through the JAXA Himawari Monitor along with the Himawari Standard Data provided by JMA. The Himawari geophysical parameters are produced in NetCDF4 format and provided to registered users by FTP in near-real-time basis.Currently, we are developing new geophysical parameters to be distributed through the system. Ocean color (suspended substances and chlorophyll-a), Photosynthetic Active Radiation (PAR), and cloud properties (cloud top temperature, optical thickness, and effective particle radius) data are planned to release to public in 2016.

Keywords: Himawari-8, Sea surface temperature, aerosol property, ocean color, cloud property

Investigating impact of subpixel horizontal inhomogeneity on retrieval of cloud microphysical parameters from multi-spectral imagers

*Takashi M. Nagao[1], Takashi Y. Nakajima[2], Husi Letu[3], Hiroshi Murakami[1]

1.Earth Observation Research Center, Japan Aerospace Exploration Agency, 2.Tokai University Research and Information Center, 3.Institute of Remote Sensing and Digital Earth, Chinese Academy of Sciences

The importance of cloud in terrestrial atmospheric dynamics and radiative transfer as key elements of the water and energy cycles have motivated development of various remote sensing technics for monitoring cloud microphysical parameters by using satellite-borne multispectral imagers (e.g. MODIS/Aqua). We have been developed a cloud retrieval algorithm for the Second Generation Global Imager (SGLI) onboard a new earth observation satellite, the Global Change Observation Mission-Climate (GCOM-C), that Japanese Aerospace Exploration Agency (JAXA) is scheduling to launch in Japan fiscal year 2016. The SGLI instrument is a radiometer providing near-ultraviolet-to-thermal-infrared multi-spectral measurements at 250 m, 500 m or 1 km resolutions. The algorithm can retrieve cloud optical thickness (COT), cloud particle effective radius (CER), and cloud top temperature (CTT) simultaneously from visible and infrared measurements at three spectral bands of the SGLI. And then, we are also working on applying our algorithm to the measurements from the Advanced Himawari Imager (AHI) onboard the Japan Meteorological Agency's geostationary meteorological satellite, Himawari-8.The AHI is also a radiometer providing visible-to-thermal-infrared multi-spectral measurements of every 2.5 minutes for Japan area and 10 minutes for full disk at 500 m, 1 km or 2 km resolutions. Therefore, retrievals of cloud parameters derived from both SGLI's global high-resolution observations and AHI's high-frequency observation will be obtained. However, there may be discrepancies between retrievals from the SGLI and AHI. As pointed out by previous studies, cloud retrievals are impacted significantly by vertical and horizontal distribution of cloud properties. And the impact on retrievals depends on the spectral characteristics, the spatial resolution and the observation angles of the instruments. This study focuses on bias in cloud retrievals caused by both horizontal inhomogeneous cloud properties and clear-region-contamination at subpixel scale. First, we introduce our cloud retrieval algorithm for the SGLI and show the comparison of cloud retrievals obtained by applying our algorithm to the MODIS's (instead of SGLI's) 1 km resolution observations and the AHI's 2 km resolution observations. Second, we simulate biases in COT, CER and CTT retrievals for various spatial resolution observations including SGLI's and AHI's observations by using high-spatial resolution (30 m) measurements of the Landsat-8. The simulation result explains the relationship between cloud horizontal inhomogeneity and clear-region-contamination and retrieval bias, and also suggests that the bias can be estimated by using co-variance matrix of multi-spectral radiances within the target pixel. Finally, the possibility of estimating the bias from SGLI's and AHI's observation themselves is discussed.

Keywords: GCOM-C, Himawari-8, Cloud property

Retrieval of the ice cloud properties from MODIS and HIMAWARI-8 satellite measurements by Voronoi ice particle scattering model

*Husi Letu[1,2], Takashi M. Nagao[3], Hiroshi Ishimoto[4], Takashi Y. Nakajima[2], Riedi Jerome[5], Huazhe Shang[1], Liangfu Chen[1]

1.Institute of Remote Sensing and Digital Earth, Chinese Academy of Sciences (CAS), China, 2.Research and Information Center (TRIC), Tokai University, Japan, 3.Earth Observation Research Center (EORC), JAXA, Japan, 4.Meteorological Research Institute, Japan, 5.5 Laboratoire d'Optique Atmosphérique, Université de Lille, France

Ice clouds play an important role in the radiation balance of the Earth's atmospheric system through interaction with solar radiation and infrared emission. However, there are still large uncertainties in characterizing their microphysical and optical properties, due to their complex habit. In this study, single scattering property of the aggregated ice cloud particle called Voronoi habit model is developed for applying in the ice cloud radiative transfer simulations and retrieval of their optical and microphysical properties. A combination of the finite- difference time-domain (FDTD) method, Geometric Optics Integral Equation (GOIE) technique, and geometric optics method (GOM) are applied to compute the single scattering properties of the Voronoi model. The POLDER multi-angles measurements are employed to evaluate the efficiency of the Voronoi model on retrieval of the ice cloud properties. The CAPCOM cloud property retrieval algorithm is improved to retrieve the ice cloud properties for MODIS and HIMAWARI-8 satellite measurements based on the Voronoi model. Optical thickness and effective particle radius of the ice clouds are retrieved from Aqua/MODIS data using the CAPCOM and Voronoi models. The inversion results by Voronoi model and the CAPCOM algorithm are compared to MODIS collections-6 ice cloud products for investigating the retrieval results by the Voronoi models. Ice cloud properties are also retrieved from the HIMAWARI-8 satellite data. In this presentation, we will also introduce the some results of the ice cloud retrievals by Voronoi model and characteristics of the ice cloud properties in Asia-Pacific region.

Keywords: Ice cloud, Particle scattering property, Microphysical property

Variations of Ocean Vortex Train of Green Island from Satellite Imagery

*PoChun Hsu[1], ChenChih Lin[1], ChungRu Ho[1]

1.Department of Marine Environmental Informatics, National Taiwan Ocean University, Keelung, Taiwan

Kuroshio, a western boundary current, flows quickly and steadily along the east coast of Taiwan. The ocean vortex train induced by the Kuroshio on the leeside of Green Island, which is a small islet at the path of Kuroshio off southeast Taiwan, is investigated in this study. The horizontal scale and characteristics of the ocean vortex train are analyzed with five kinds of satellite imagery, including optical imagery from SPOT (Satellite Pour l'Observation de la Terre) and Formosat-2 satellites, as well as synthetic aperture radar imagery from ERS-2 (European remote sensing satellite), ALOS (Advanced Land Observing Satellite), and Sentinel-1. Satellite altimetry data and moored acoustic Doppler current profiler (ADCP) are used to calculate the velocity of Kuroshio. The ADCP data show that the velocity is enhanced on the left of the vortex train when it is formed on the leeside of Green Island. The data derived from MODIS (Moderate-resolution Imaging Spectro-radiometer) also show that the sea surface temperature of recirculation water is more than 2^{o}C colder and the chlorophyll-a concentration is two times higher than the surrounding waters. Wind forcing may affect the vortex train obviously. The averaged aspect ratio and dimensionless width of vortex train derived from available satellite images are 2.09 and 2.02, respectively for the cases of southerly, and are 1.91 and 2.76, respectively for the cases of northerly.

Keywords: Kuroshio, Green Island, vortex train, satellite imagery

Development of new satellite ocean colour products: moving forward to an estimation of phytoplankton photo-physiology

*Takafumi Hirata[1], Koji Suzuki[1]

1.Faculty of Environmental Earth Science, Hokkaido University

Since the launch of the Coastal Zone Color Scanner (CZCS) in the 1970s, ocean color remote sensors have been providing synoptic views of marine biological (and biogeochemical) activities via surface chlorophyll-a observation. The ocean colour algorithms, in addition to ocean colour sensors, also evolved since the CZCS, and the remote sensing data of various biogeochemical variables have become available (e.g. particulate organic carbon, calcite concentration, chromophoric dissolved organic matter etc.). While availability of the biogeochemical products from the ocean color remote sensing is continuously growing, it is only the fluorescence line height due to phytoplankton that became available as a biological product after chlorophyll-a. Here we challenge to develop a new satellite algorithm to retrieve more biological variables using the ocean colour remote sensing. We found in theory that some physiological quantities of various phytoplankton groups such as the chlorophyll-a specific-absorption coefficient and the quantum yield of photosynthesis can be retrieved by integrating a bio-optical theory and an image processing technique. When these biological products were actually derived using the satellite ocean colour data, our analyses revealed that primary productivity of some phytoplankton groups could be largely influenced by their physiology rather than their biomass. This implies the importance of physiological observation of phytoplankton for a better understanding of ocean biogeochemical processes and ecology.

Keywords: ocean color remote sensing, phytoplankton, photo-physiology

Improvement of GCOM-C chlorophyll-*a* concentration product by in-situ optical measurements

*Hiroshi Murakami[1], Yoko Kiyomoto[2], Hiroaki Sasaki[2]

1.Earth Observation Research Center, Japan Aerospace Exploration Agency, 2.Seikai National Fisheries Research Institute, Fisheries Research Agency

Global Change Observation Mission for Climate (GCOM-C) which carries Second-generation Global Imager (SGLI) is planned to be launched in Japanese Fiscal Year (JFY) 2016 (from April 2016 to March 2017). SGLI has middle spatial resolution (250 m to 1000 m), wide swath (1150 km to 1400 km), 19 bands from near-UV (380 nm) to thermal infrared (12 um) wavelengths, and two-channel (red and near infrared) slant view polarization observations. SGLI will provide several ocean color products including normalized water-leaving radiance (*NWLR*) (or remote sensing reflectance (R_{rs})), photosynthetically available radiation (*PAR*), chlorophyll-*a* concentration (*Chla*), colored dissolved organic matter (*CDOM*), total suspended matter concentration (*TSM*), which will contribute to coastal environment monitoring and climate researches by the SGLI 250m resolution and wide swath. *Chla* is a key parameter to know phytoplankton distribution and the ocean primary production. Traditionally, it was estimated by an empirical regression between *Chla* and blue/green ratio of Rrs (e.g., OC4 algorithm (O'Reilly et al., 2000)). The regression is basing on a global in-situ dataset (e.g., NASA bio-Optical Marine Algorithm Data set, NOMAD (Werdell and Bailey, 2005)). However, the relationship can be deviated due to anomalous condition of inherent optical properties (IOPs), phytoplankton absorption, a_{ph}, CDOM + detritus absorption, a_{dg}, and particle back-scattering, b_{bp}, especially in the coastal areas.
This study showed improvement of the *Chla* estimation by considering the IOP deviation through a simple IOP models (Gordon et al., 1988 and Lee et al., 2002). We tested the scheme for in-situ Rrs and *Chla* data observed by Seikai National Fisheries Research Institute (SNFRI) in the East China Sea, which is independent of the NOMAD dataset. Firstly, we calculated $Chla^{1st}$ by the traditional OC4 algorithm and a_{ph} by the linear matrix inversion scheme (Hoge and Lyon, 1996, 1999) from the observed R_{rs}. Then, R_{rs} is modified by the IOP model with the estimated a_{ph}, which is assumed to be strongly related to *Chla*, and average state of a_{dg} and b_{bp} at condition of the *Chla* value. The average state of a_{dg} and b_{bp} was modeled by regression with *Chla* basing on the NOMAD dataset in advance. Finally we recalculated $Chla^{re}$ by the OC4 algorithm applied to the modified R_{rs}. Mean absolute difference (MAD) compared to the in-situ observed *Chla* was improved from 50% ($Chla^{1st}$) to 40% ($Chla^{re}$).
This scheme assumed spectral shape of a_{ph}, a_{dg} and b_{bp}, however they can change in various coastal environment. Collection of the in-situ bio-optical measurements in the various coastal areas is required to develop more robust GCOM-C algorithms and methodology to estimate coastal *Chla*.

Keywords: GCOM, GCOM-C, SGLI, ocean color, chlorophyll-a concentration

Application of Bio-Optical Model and Satellite Image in Identification and Mapping of Submerged Macrophytes in South-Basin of Lake Biwa, Japan

*Shweta Yadav[1], Yosuke Yamashiki[1], Minoru Yoneda[1], Tamura Masayuki[1], Suzaki Junichi[1], Kanako Ishikawa[2]

1.Kyoto University, 2.Lake Biwa Environmental Research Institute (LBERI)

Abstract

Aquatic macrophytes are important for primary production and environmental protection of marine and fresh water ecosystems. However excessive growth of macrophytes may cause an adverse shift in shallow lakes from clear-water plant-dominated states to turbid algae-dominated state. In order to effectively manage the inland waters and their ecosystem, it is crucial to monitor the community structure and distribution of aquatic macrophytes.

Present study focus on identifying and mapping the submerged macrophyte species dominated in eutrophic south basin of Lake Biwa, using satellite image (Landsat) and bio-optical model. Spectral signature of various submerged macrophytes were generated. Laboratory experiments were conducted to identify the reflectance spectra of the macrophytes at different wavelength, using FieldSpec Spectroradiometer. Result indicates that visible (450-670 nm) and near-infrared (850-880 nm) bands are the significant for spectral discrimination of submerged macrophytes. Image processing software Erdas-Imagine-2013 was used to map the macrophytes species.

Keywords: Remote Sensing, Bio-Optical Model, Submerged Macrophytes, Mapping

Satellite Retrieval of Overstory and Understory Leaf Area Index in High Northern Forests

*Wei Yang[1], Hideki Kobayashi[2], Kenlo Nishida Nasahara[3]

1.Center for Environmental Remote Sensing, Chiba University, 2.Japan Agency for Marine-Earth Science and Technology, 3.University of Tsukuba

Leaf area index (LAI), defined as one-half the total green leaf are per unit of horizontal ground surface area, is a crucial input parameter for global carbon cycle modeling. Since carbon fixed through net primary productivity has different residence times for different components, the LAI for overstory and understory vegetation in forest ecosystems need to be treated differently in carbon cycle modeling. Currently, satellite remote sensing is the only feasible technique to measure the LAI at a continental and/or global scale over a long periods of multiple years. However, there are no existing satellite products that provide simultaneous estimation of overstory and understory leaf area index (LAIo and LAIu) at present. Consequently, we proposed an integrating look-up table (LUT) method to remotely estimate the LAIo and LAIu for boreal forests, where are encountering rapider temperature change than other areas. In the newly proposed method, the understory normalized vegetation difference index (NDVIu) is first retrieved from multiple satellite observations by using a semi-empirical method. Then the LAIu is estimated from the retrieved NDVIu through searching a LUT generated by radiative transfer simulation for understory vegetation. In order to estimate the LAIo, a new land-cover map of forest types, which classifies the boreal forests as low, medium and high types, is generated by using a wall-to-wall canopy height product to replace the conventional global land-cover maps. The LUTs containing angles, LAIu, LAIo, and corresponding reflectance at red and near-infrared bands are generated for each forest type by running a radiative transfer model. Specifically, the forest landscape parameters are determined by an empirical forest structure model. Moreover, the retrieved NDVIu is used as an ancillary information to constrain the relationship between LAIo and canopy reflectance. The validation results showed acceptable accuracy based on our filed measurement at interior Alaska, America.

Keywords: Satellite Remote Sensing, Leaf Area Index, Northern Forests

Hyperspectral Imaging from International Space Station : Hyperspectral Imager Suite (HISUI)

*Tsuneo Matsunaga[1], Satoru Yamamoto[1], Toru Sakai[1], Akira Iwasaki[2], Satoshi Tsuchida[3], Koki Iwao[3], Jun Tanii[4], Osamu Kashimura[4], Hirokazu Yamamoto[3], Koichiro Mouri[4], Tetsushi Tachikawa[4]

1.National Institute for Environmental Studies, 2.The University of Tokyo, 3.National Institute of Advanced Industrial Science and Technology, 4.Japan Space Systems

Hyperspectral Imager Suite (HISUI) is a spaceborne imaging spectrometer being developed by Ministry of Economy, Trade, and Industry (METI) of Japan for the deployment on International Space Station (ISS) Japan Experiment Module (JEM) in FY2018. It will be METI's fourth spaceborne optical imaging system after JERS-1 OPS (1992 –1998), ASTER (1999 -), and ASNARO-1 (2014 -). HISUI has one reflective telescope, two grating spectrometers, two area detectors, and a mechanical cooler, and covers 0.4 - 2.5 μm spectral region with 185 spectral bands, 20 m (cross track) x 30 m (along track) spatial resolution, and 20 km swath, from the altitude of 400 km. The basic specifications of HISUI are summarized in Table 1.

HISUI project is currently being promoted by three organizations each of which has a contract with METI : Japan Space Systems, NEC Corporation, and National Institute of Advanced Industrial Science and Technology (AIST). In addition, several scientists from universities and national research institutes are participating in the HISUI project.

The planned operation of HISUI onboard ISS will be three years from 2019. In this time period, ISS will have several advanced earth observing instruments such as a vegetation lidar (Global Ecosystem Dynamics Investigation, GEDI), a thermal camera for terrestrial vegetation (ECOsystem Spaceborne Thermal Radiometer Experiment on Space Station, ECOSTRESS) and a carbon dioxide sensor (Orbital Carbon Observatory 3, OCO-3). Synergy among these instruments will provide us new information on terrestrial ecosystem which cannot be obtained from indivisual observations by these instruments. Especially, simultaneous observation by GEDI and HISUI will enable combined analysis of biomass amount data from a lidar and physiological parameters of vegetation from an imaging spectrometer.

Table 1. HISUI Specifications.

Spatial resolution	20 m (CT) x 30 m(AT)
Swath	20 km
Spectral coverage	0.4 - 2.5 μm
Spectral resolution	10 nm (VNIR) 12.5 nm (SWIR)
Number of band	185
Signal to noise ratio	>450 @ 620 nm >300 @ 2100 nm
MTF	> 0.2
Dynamic range	12 bits
Data compression	Lossless (70%)
Pointing capability	≈±5 ° (±35 km)
Data rate (70 % compression)	0.4 Gbps
Maximum data amount per day	690 Gbyte

The altitude of ISS is assumed to be 400 km.

The current status of GOSAT and GOSAT-2

*Tsuneo Matsunaga[1], Tatsuya Yokota[1], Masakatsu Nakajima[2], Gen Inoue, Ryoichi Imasu[3]

1.National Institute for Environmental Studies, 2.Japan Aerospace Exploration Agency, 3.The University of Tokyo

Greenhouse Gases Observing Satellite (GOSAT) and its successor, GOSAT-2, are Japanese earth observing satellites for greenhouse gases measurements from space. Both satellite projects are joint efforts among Ministry of the Environment (MOE), Japan Aerospace Exploration Agency (JAXA), and National Institute for Environmental Studies (NIES).
GOSAT was launched in January 2009, already finished its design lifetime (five years), and is currently in its extended operation period. Its data have been used to calculate whole-atmosphere monthly mean carbon dioxide concentration and to identify locations with large anthoropogenic emissions of CO2 and methane.
GOSAT-2 will be launched in FY2017. Both satellites have Fourier transform spectrometers for the measurements of columnar abundances of greenhouse and other gases and UV-VIS-NIR-SWIR imagers for cloud and aerosol detection. GOSAT-2 instruments (FTS-2 and CAI-2) will be modified or improved based on the experiences of GOSAT instruments (FTS and CAI). FTS-2 will have the extended spectral coverage for carbon monoxide measurement and the intelligent pointing capability to avoid cloud contamination. CAI-2 will have multiple UV bands for more precise land aerosol monitoring and forward/backward viewing capability to avoid sun glint over oceans. Most of critical design reviews of GOSAT-2 spacecraft, earth observing instruments, and ground systems have been completed.

Synergistic observations using a wide spectral-coverage FTS and an agile pointing mechanism onboard GOSAT

*Akihiko Kuze[1], Hiroshi Suto[1], Kei Shiomi[1], Fumie Kataoka[2], Jun Yoshida[3]

1.Japan Aerospace Exploration Agency, 2.Remote Sensing Technology Center of Japan, 3.NEC cooperation

Since February 2009, Thermal And Near infrared Sensor for carbon Observation Fourier-Transform Spectrometer (TANSO-FTS) onboard the Greenhouse gases Observing SATellite (GOSAT) has been providing long-term high-resolution radiance spectra of and uniform quality. Among the satellite-borne spectrometers for greenhouse gases (GHG) observations, only GOSAT uses FTS technology to acquire high-resolution spectra. With the FTS multiplex advantage, the single spectrometer with a common field of view can simultaneously cover both two linear polarization of the solar scattered light and thermal emission from the earth's surface and atmosphere. After seven years of operation, most of the level 2 products have still been retrieved only from the scalar solar scattered light spectra. However, there is a strong need to acquire information for at least two vertical-layers (upper and lower atmosphere) to understand GHG dynamics. Theoretically, vertical profiles can be retrieved from thermal infrared spectra using the Levenberg-Marquardt method. The algorithm assumes that the measurements and a priori errors are random; however, actually measured radiance spectra and the forward model show calibration errors and systematic biases, respectively. In addition, in the existing retrievals, many parameter need to be retrieved simultaneously. These errors make retrievals unstable. Therefore, the parameters to be assumed and retrieved need to be reconsidered.
The modification of the light path by the scattering induced by thin clouds and aerosol scatterings, which are highly polarized, is still the largest source of errors and information on their vertical location can minimize the errors in GHG retrievals. The measured light is a combination of surface reflection and scattering by clouds and aerosols, which have different phase functions. Polarization measurement of O_2 A band spectra has potential height information The TANSO-FTS instrument has a ZnSe non-coated beam with an incident angle of 45deg and a large polarization sensitivity. The analysis using vector radiative transfer calculation and an instrument Muller matrix becomes complicated. The polarization of the spectra shows strong dependency on the geometry of the sun, the target object and the satellite. A unique function of TANSO-FTS is agile targeting; the two axes mechanism helps target and view a point source from different geometries by uploading the pointing angle and location tables on a daily basis.
In this study, a simpler but robust algorithm is proposed by minimizing the number of parameters to be retrieved, and optimizing sampling pattern and viewing geometry to minimize the highly geometry-dependent polarization related errors.

Keywords: GOSAT , TANSO-FTS, FTS, thermal infrared, polarization, vertical profile

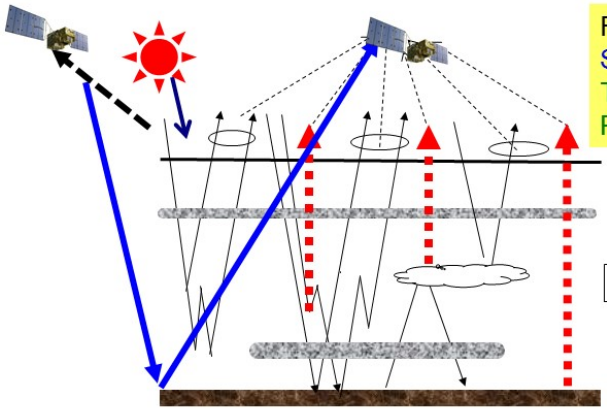

FTS covers wide spectral range
SWIR: near surface information
TIR and O_2A profile information
Polarization: scattering information

High spectral resolution data of (1) Solar lines (Fraunhofer lines, Fluorescence)
(2) Earth albedo (reflectance and scattering)
(3) Thermal radiation
(4) Two linear polarizations

Validation of the GSMaP Gauge NRT

*Tomoaki Mega[1], Tomoo Ushio[1]

1.Graduate School of Engineering, Osaka University

Information of real time precipitation is important for water disaster management. However real-time observation does not cover the whole world. Satellite observes global precipitation, although a satellite observation is limited overpass time. Global Satellite Mapping of Precipitation (GSMaP) is hourly rainfall map using combined passive microwave and infrared radiometric data from multi satellite. GSMaP in near-real-time (NRT) is providing data 4-hour after observation. Precipitation retrieval from the passive microwave radiometer underestimate over land. Gauge adjusted GSMaP (GSMaP Gauge) achived to compensate GSMaP MVK precipitation by gauge data. The method is not applied to GSMaP NRT, because we do not get global rain gauge data in 4 hour. We developed new GSMaP Gauge adjusted GSMaP NRT (GSMaP Gauge NRT). The new method estimate adjustment parameters for GSMaP NRT using previous GSMaP Gauge and GSMaP MVK. The method modify precipitation of the GSMaP NRT with these parameters. Distribution of monthly precipitation of GSMaP Gauge NRT is close to that of GSMaP Gauge. We will introduce GSMaP Gauge NRT algorithm and present validation of the GSMaP Gauge NRT.

Keywords: precipitation, microwave radiometer, GSMaP

Evaluation of the rain rate estimates of GPM/DPR using ground radar data

*Tatsuya Shimozuma[1], Shinta Seto[1]

1.Nagasaki University

1. Introduction

GPM (Global Precipitation Measurement) Core Observatory satellite has been in operation since February, 2014. GPM Core Observatory satellite is equipped with the Dual-frequency Precipitation Radar (DPR), the DPR consists of a Ku-band precipitation radar (KuPR) and a Ka-band precipitation radar (KaPR). The observation made with the spaceborne radar DPR is the first trial, and the evaluation is needed for the observation results. In this study, we focus on matchup cases with the XRAIN ground radar, and compare the rain rate estimates by DPR and XRAIN. Moreover, we discuss the reason of difference in the rain rate estimates.

2. Method

The Ministry of Land, Infrastructure, Transport and Tourism (MLIT) built the rainfall observation radar network called XRAIN. High frequency (every 1 minute) and high resolution (250m mesh) measurement becomes possible in comparison with a conditional ground radar. And XRAIN is operated at 39 places in Japan as of February 2016. And XRAIN is operated at 14 places in Japan as of February 2016. In this study, we focus XAIN radars to be operated in northern Kyushu region. Observation resolution is not same between DPR and XRAIN. The average is calculated from the XRAIN's rain rate included in DPR's footprint, and the rain rate estimates by DPR and XRAIN are compared. We used the DPR's rain rates at the clutter free bottom, which is stored as the variable name of [precipRateNearSurface]. The product version of DPR is V03B.

3. Comparison of the rain rate estimates between DPR and XRAIN

The rain rate estimates are compared between DPR and XRAIN. As DPR and XRAIN make different observation area, their match-up data that satisfy the following conditions, (1) the observation area is overlap, (2) some degree of rain rate is observed, were extracted. 50 matchup cases of DPR and XRAIN are found between June 2014 and January 2016. In this section, a match-up data at 03:27 (JST) of July 7th, 2015 (DPR orbit number:7703) is presented. The rain rate estimates of DPR and XRAIN are shown in Fig.1. The rain rate estimates of XRAIN are overestimated, and the area where rain is detected are different. The linear distribution are found in XRAIN's rain rate. The scatterplot of the rain rate between XRAIN and DPR is shown in Fig.2. X-axis is XRAIN's rain rate, and Y-axis is DPR's rain rate. Red symbols are for stratiform rain and blue symbols are for convective rain. From Fig.2, observation data that surrounded by XRAIN side show that XRAIN's estimates are higher than DPR's estimates. And the bias is negative value.

4. Comparison of the rain rate estimates in 50 matchup cases between DPR and XRAIN

In this section, the rain rate estimates of 50 matchup cases are evaluated. 2-D histogram of the rain rates between XRAIN and DPR is shown in Fig.3. Red line shows DPR's average rain rate estimates for XRAIN. From the Fig.3, the rain rate estimates of XRAIN are overestimated. And the average line is high in XRAIN rain rate over 0.6mm/hr. The factors of the differences are (1) measurement height is not same and (2) the estimation accuracy decrease as far from the central point of the radar. As DPR can provide the 3-dimensional rain rate distribution, in the future, we will compare the rain rate estimates at the same height.

5. Conclusion

GPM Core Observatory satellite has been in operation since February 2014. The observation made with DPR is the first trial, and the evaluation is needed for the observation results. We focus on the observation result of the XRAIN, and compare the rain rate estimates by DPR and XRAIN. As a result

of comparison, the rain rate estimates of XRAIN are overestimated. The factors of the differences are focus height and distance from the ground radar. In the future, we will compare the rain rate estimates at the same height.

Keywords: Global Precipitation Measurement (GPM), Dual-Frequency Precipitation Radar (DPR), MLIT X-Band MP Radar Network (XRAIN)

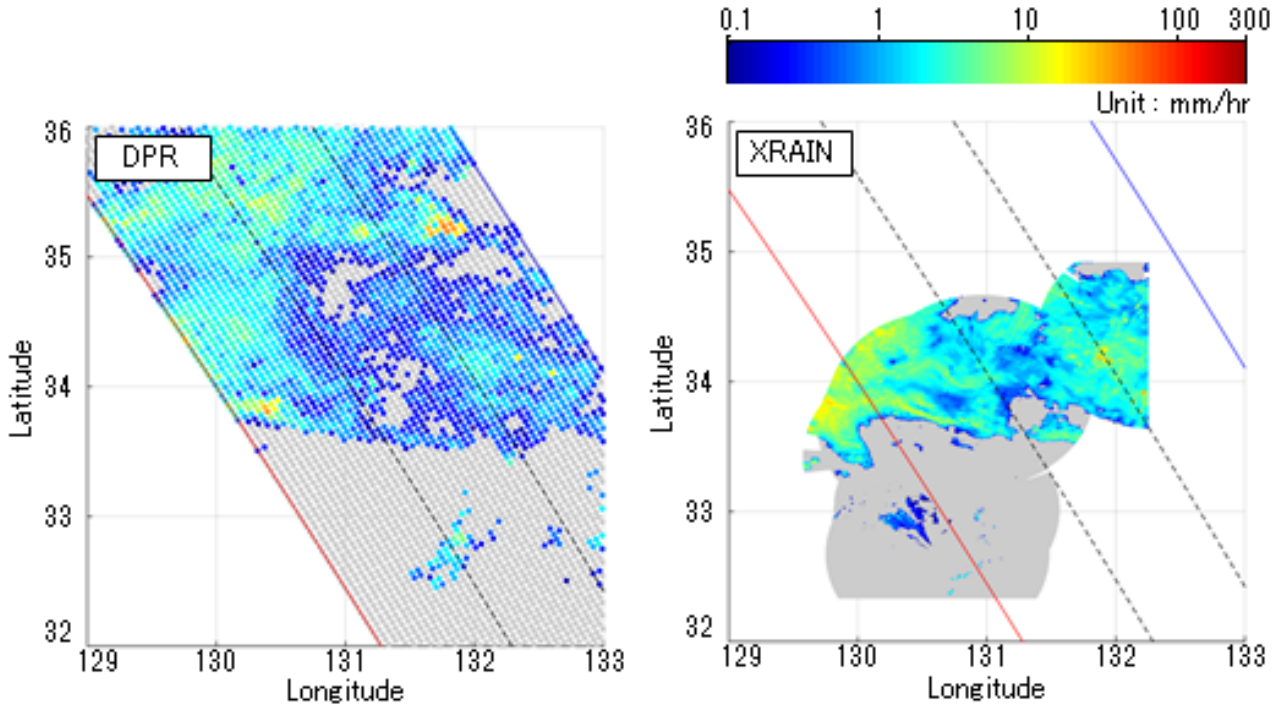

Fig.1 The rain rate estimates

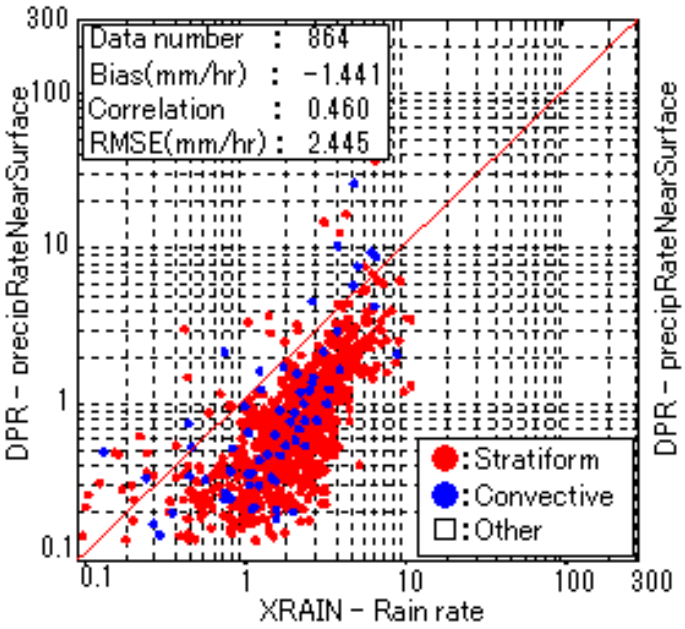

Fig.2 Scatterplot of the rain rate

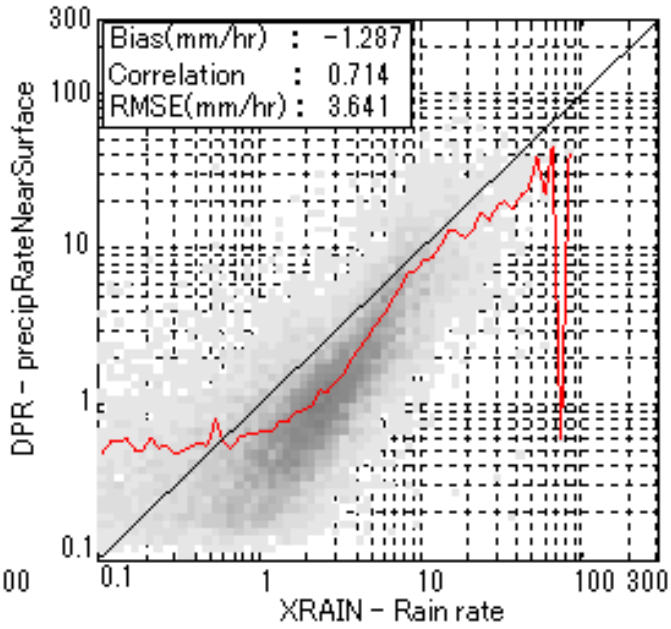

Fig.3 2-D histogram of the rain rate

A difference in the interannual variability of precipitation between PR and TMI

*Kaya Kanemaru[1], Takuji Kubota[1], Misako Kachi[1], Riko Oki[1], Toshio Iguchi[2], Yukari Takayabu[3]

1.earth observation research center, japan aerospace exploration agency, 2.National Institute of Information and Communications Technology, 3.Atmosphere and Ocean Research Institute, University of Tokyo

Precipitation has an important role in maintaining the hydrological cycle on the earth's climate, so that understanding the long-term variability of precipitation is essential to provide for the future such as the decadal climate variability or the climate change. It is, however, well known that the interannual variability of precipitation associated with El Nino Southern Oscillation (ENSO) is different between the Tropical Rainfall Measuring Mission (TRMM) Precipitation Radar (PR) and the TRMM Microwave Imager (TMI) estimates (Robertson et al. 2003; Wang et al. 2008; Lau and Wu 2011). The current study is aimed to explore the origin of the difference of the interannual variability of precipitation between PR and TMI.
The current study focuses on the differences in the precipitation type (convective and stratiform types) and its interannual variability. The precipitation estimates derived from PR (2A25; Iguchi et al. 2009) and TMI (2A12; Kummerow et al. 2011) products are individually divided into stratiform and convective precipitation estimates. The PR product contains results of the precipitation type in each pixel, but the TMI product contains together in same pixel. These data are projected onto a common 0.5 degrees gridded instantaneous data with ascending and descending orbits and sampled only where PR and TMI observations are available. Data are analyzed in the El Nino season (December 1997 to May 19998) and the La Nina season (December 1999 to May 2000) and compared between PR and TMI. Differences in unconditional precipitation average of convective and stratiform types over semi-global (35S-35N) oceans are overall same between PR and TMI in the La Nina season, because the database for the TMI retrieval was generated by means of the PR observation in this period. On the other hand, the difference in the convective precipitation between PR and TMI (TMI is generally higher than PR) are obviously found in the El Nino season, while the stratiform precipitation is similar between PR and TMI. The regions where the difference in convective precipitation between PR and TMI are large are found in warm sea surface temperatures (SSTs) for 300 to 303 K and moist column water vapors (CWVs) for 66 to 75 mm and frequently located over the central Pacific in the El Nino season. In the El Nino event, the ratio of stratiform precipitation against total precipitation central Pacific was increased (Schumacher and Houze 2003), which implies that the TMI does not follows the interannual nature-variability of the precipitation characteristics observed by the PR.

Keywords: Precipitation Radar, Microwave radiometer, Interannual variability

Additional information of precipitating cloud life stages for Improvement of rain rate data estimated from Himawari-8

*Hitoshi Hirose[1], Atsushi Higuchi[1], Tomoaki Mega[2], Tomoo Ushio[2], Munehisa K Yamamoto[3], Shoichi Shige[3], Atsushi Hamada[4]

1.Center for Environmental Remote Sensing, Chiba University, 2.Department of Engineering, Osaka University, 3.Department of Science, Kyoto University, 4.Atmosphere and Ocean Research Institute, The University of Tokyo

Rain observation with microwave radiometer satellites is essential to make global rain observation data with high temporal resolution. However microwave satellites cannot cover a global area since the number of them is limited. In such an area where no microwave satellite is available, improvement of rain estimation accuracy is expected by using rain information obtained from geostationary meteorological satellites (GMS) with high temporal resolution. Kühnlein et al. (2014) reported that they could estimate rain with high temporal resolution same as GMS by using a statistical method called Random Forest (RF) , which 10 channels information of brightness temperature observed from METEOSAT Second Generation (MSG-2) GMS are associated to truth of rain observed from ground-based radar. In this method, first some channels are selected from among GMS observations to make a classification tree deciding rain or no rain areas. Then the number of tree is increased in the same way, and finally rain or no rain area is decided by majority of all tree's results. In addition rain type classification and rain rate estimation are possible by the RF method. This study produced a new rain estimation product with high temporal resolution by applying this RF method to the only third generation GMS, Himawari-8 for compensating the lack of microwave satellites observation network. Moreover we used the Global Precipitation Measurement (GPM) main satellite instead of ground-based radar for the truth of rain used in machine learning for expanding the analysis area to all of the Himawari-8 observing area.
For verification of the above product, the threat score of the rain area estimated from Himawari-8 was calculated by comparing with rain observed by ground-based radar in near Japan region as the truth. As a result, the threat score in daytime is very high value more than 0.5, and that in night time is more than 0.42, which are conditionally comparable to microwave rain estimation. Next we verified effectiveness of Himawari-8 new additional channels to rain estimation. Then in rain area classification, a visible blue channel (0.46μm) is most effective and in rain type classification a near Infrared channel (1.6μm) is most effective. Route mean square error of rain rate is about 1.3 mm par hour but strong rain greater than 8.0 mm par hour is tend to be underestimated. This is partly because that it is difficult to distinguish thick convective cloud from thin cirrus since the rain rate estimated by RF method is mainly based on cloud top temperature (height) information obtained from Himawari-8 observation of brightness temperature. To overcome this problem, we tried to improve an accuracy of estimating convective rain rate by using temporal variation information of rainy cloud. First a moving vector of rainy cloud is calculated from every 10 minutes global observation of Himawari-8. Next we added temporal variation information of rainy cloud brightness temperature obtained by tracing rainy cloud with the moving vector into the RF method. As a result the Himwari-8 rain rate product is improved with life stage information of rainy cloud. We intend to show example analysis of the improved Himawari-8 rain product in near Japan region.
Himawari-8 GMS data is released from the Center for Environmental Remote Sensing, Chiba University. We used near surface rain observed by GPM (Ku PR) and rain intensity observed by ground-based radar in the Japan Meteorological Agency as the truth of Rain

Keywords: Himawari-8, GPM, precipitation, GSMaP

Climatological Cloud Database Estimated by Geostationary Satellite Split-Window Measurements

*Noriyuki Nishi[1], Atsushi Hamada[2], Hitoshi Hirose[3], Hitoshi Mukougawa[4]

1.Faculty of Science, Fukuoka Universtiy, 2.AORI, University of Tokyo, 3.CEReS, Chiba University, 4.Disaster Prevention Research Institute, Kyoto University

We extended our cloud-top database spatially to the midlatitude and temporally to new satellite Himawari-8. We have already released a database of cloud top height and visible optical thickness (CTOP) with one-hour resolution over the tropical western Pacific and Maritime Continent, using infrared split-window data of the geostationary satellites (MTSAT-1R and MTSAT2) (http://database.rish.kyoto-u.ac.jp/arch/ctop/). By comparing MT-SAT IR observation and the direct observation of the cloud top height by CloudSat radar, we can construct a lookup table (LUT) with which the cloud top height is estimated by using only MTSAT data. Unfortunately, now in the age of Himawari-8 that has been available since July 2015, the CloudSat observations are limited in the daytime and the precise direct comparison with the data cannot be conducted to construct LUT. Therefore, we proceeded an alternative way by constructing a calibration table based on the comparison between MTSAT-2 and Himawari-8 observations during July 2015 when both geostationary satellites were in operation. By using the similar approach repeatedly, it will be possible to construct LUT for the past geostationary satellites that had been in operation before the launch of CloudSat in 2006.
We also tried to extend the targeted region to the mid-latitude. In our present scheme applicable for only tropics, the vertical profile of temperature is assumed to be almost constant in whole tropics and all the year. However, since the temperature variability is much larger in mid latitude, it is not plausible to assume that the same IR radiance comes from the clouds with a certain top height. Therefore, we proposed a new method to use temperature data of the global analysis together. The temperature of the cloud top is estimated through the altitude of the cloud top observed by CloudSat as well as the temperature profile deduced from the global analysis data. Then we constructed LUT of cloud top temperature (not height) by the regression of the MTSAT IR radiance with respect to cloud top temperature. We can get the cloud top height at any point at any time by converting the cloud top temperature to cloud top height, with using global analysis data. A preliminary estimate using this method indicated that the cloud top height is estimated within allowable error even in the mid latitude.

Keywords: geostationary satellite, cloud, database

Simultaneous retrieval of aerosol optical thickness and chlorophyll concentration using multi-wavelength and multi-pixel method

*CHONG SHI[1], Teruyuki Nakajima[1], Makiko Hashimoto[1], Hideaki Takenaka[1]

1.JAXA/EORC

This study proposes an algorithm for the simultaneous retrieval of aerosol optical thickness(AOT) and chlorophyll concentration using multi-wavelength and multi-pixel method over ocean. In our algorithm, the forward radiation calculation is performed by a coupled atmosphere-ocean model(Ota et al., 2010; Nakajima and Tanaka, 1986) with an improved bio-optical ocean module(Shi et al., 2015) for CASE 1 water, which is different to the traditional ocean color algorithms which decouple the atmosphere and ocean surface(Gordon and Wang, 1994) using atmospheric correction procedures; then the Maximum a posterior method(Rodger, 2000) but considering the spatial constrain incorporated with the multi-pixel optimization algorithm(Hashimoto, 2014) is used to retrieval aerosol optical thickness and chlorophyll concentration. For the AOT retrieval, a global aerosol transport-radiation model named SPRINTARS(Takemura et al,. 2000) is used as the priori constrain; Finally, the inversion results are achieved from HIMAWARI-8 and GOSAT-TCAI satellite observation data through comparison to AERONET products and other aerosol retrieval algorithm which is widely used in satellite remote sensing.

Keywords: Aerosol, Ocean color, Remote sensing, Radiative transfer

Simultaneous observations of solar-induced chlorophyll fluorescence by vegetation and atmospheric CO_2 dynamics by GOSAT

*Hibiki M Noda[1], Kouki Hikosaka[2], Kazutaka Murakami[1], Tsuneo Matsunaga[1]

1.NIES National Institute of Environmental Studies, 2.Tohoku University

In these decades, global warming has progressed owing to increase of greenhouse gases (GHGs) such as CO_2. To deal effectively with this issue by mitigation and adaptation, it is necessary to monitor emission and sequestration of GHGs with their underlying mechanisms including biogeochemical processes and human activities. Terrestrial ecosystem, which is the large carbon sink, absorbs 123 Pg carbon per year through plant photosynthesis (IPCC 2014). Satellite remote sensing has been used to monitor the spatial and temporal dynamics of terrestrial ecosystems that are responsible for such photosynthetic CO2 absorption. Such observation provides us with geographical information on the potential distribution of carbon sequestration by the aid of ecosystem models. However, as the photosynthesis of a given vegetation is quite sensitive to meteorological changes such as radiation, temperature and precipitation, we need to observe the photosynthetic ‘activity’ in a physiological sense, together with the atmospheric CO2 concentration over continental and global scales. Joiner et al. (2011) and Frankenberg et al. (2011) have suggested that TANSO FTS on Greenhouse Gases Observing Satellite (GOSAT) could detect overlapping part of solar-induced chlorophyll fluorescence (SIF) emitted by terrestrial vegetation and Fraunhofer line. The chlorophyll fluorescence is photons of red and far-red light that emitted by chlorophylls, and in plant ecophysiology it has been a biophysical index to examine the photosynthetic responses to environmental stresses such as extreme temperatures and drought. Thus SIF remote sensing is drawn considerable attention as a new technique to observe the photosynthetic activity of the vegetation. This paper will present our on-going and future challenges by GOSAT and GOSAT-2 to observe such photosynthetic activity of terrestrial ecosystems and its possible consequences with the atmospheric CO2 concentration from national, continental to global scales under climate change.

Keywords: carbon cycle of terrestrial ecosystem, photosynthetic production

Preliminary sensitivity study of the GOSAT-2 FTS SWIR retrievals based on the designed specifications

*Yukio Yoshida[1], Akihide Kamei[1], Isamu Morino[1], Makoto Saito[1], Hibiki Noda[1], Tsuneo Matsunaga[1]

1.NIES

The Greenhouse gases Observing SATellite (GOSAT) was launched in January 2009 and observed global distribution of the column-averaged dry air mole fractions of carbon dioxide and methane (XCO_2 and XCH_4) for about seven years. As a successor mission to the GOSAT, GOSAT-2 is planned to be launched in early 2018, and its critical design review (CDR) was completed. GOSAT-2 also has a Fourier transform spectrometer (FTS) like GOSAT to obtain short-wavelength infrared (SWIR) light reflected from the earth's surface and thermal infrared (TIR) radiation emitted from the ground and atmosphere. According to the current design of the FTS-2 (FTS onboard the GOSAT-2), its SNR is higher than or almost equal to that onboard the GOSAT, and it covers the 2.3 μm carbon monoxide (CO) band as well as the 1.6 and 2.0 μm CO_2 bands and 1.67 μm CH_4 band. Our preliminary sensitivity test shows that the SNR improvement in SWIR bands reduces the retrieval random error (precision) about 15% for XCO_2 and 35% for XCH_4 than those of GOSAT.

Keywords: GOSAT-2, XCO2, XCH4

Applied FORMOSAT-3/COSMIC on observing atmospheric temperature changes caused by volcanic eruptions

*Chun-Chieh Hsiao[1], Jann-Yenq Liu[2], Hsin I Lai[1], Yi Cheng Chiu, Shiann-Jeng Yu[1], Guey-Shin Chang[1]

1.National Space Organization, 2.Graduate Institute of Space Science, National Central University

Volcanic eruptions are often along with fiery magma, hot dense gases and powerful explosive energy. Those materials injected into atmosphere might cool tropospheric temperature and warm the temperature of bottom of stratosphere but sometimes the phenomenon was exactly opposite or mixture. This study focused on 8 volcanic eruptions, the explosive indexes of which were 4 during 2008 to 2011 and analyzed the temperature-related data from radio occultation observations of FORMOSAT-3/COSMIC (F3/C). It individually investigated the temporal latitude-altitude and longitude-altitude variances atmospheric temperatures from northeastern, northwestern, southeastern and southwestern of volcanos before and after the eruptions. This study also observed the image from Moderate resolution Imaging Spectroradiometer (MODIS) on NASA terra satellite to see where the volcanic plum extended. Results apparently show that 3 events had cooling troposphere and warming bottom of stratosphere and 2 events were just the opposite. One of the rest events was mixture case and the other one of the rest was without apparent variances in temperature. Cooling troposphere and warming bottom of stratosphere caused by stratospheric aerosols that reduced sunlight reaching troposphere and absorbed radiation at the bottom of stratosphere. The consequence opposite to above was caused by that volcanos erupted hot and high density gases into troposphere and adiabatic expansion happened during the top of troposphere and bottom of stratosphere. Moreover, in mixture case, area with more volcanic ash showed decreasing temperature in the troposphere and increasing temperature at the bottom of stratosphere. Area with less volcanic ash showed increasing temperature in the troposphere and decreasing temperature at the bottom of stratosphere.

Keywords: FORMOSAT-3/COSMIC, volcano

Cloud properties analysis based on EarthCARE/MSI observation

*Seiko Takagi[1], Takashi Nagao[2], Haruma Ishida[3], Husi Letu[4], Makiko Hashimoto[2], Takashi Nakajima[5]

1.Tokai University, Research and Information Center, 2.Japan Aerospace Exploration Agency, 3.Meteorological Research Institute, 4.Institute of Remote Sensing and Digital Earth, Chinese Academy of Sciences (CAS), 5.Tokai University, School of Information Science & Technology, Dept. of Human & Information Science

Clouds and aerosols are the major uncertainty in the understanding of the Earth’s climate system. An improvement of understanding and better modeling of the relationship of clouds, aerosols and radiation are therefore prominent part in climate research and weather prediction. It is important to obtain the global data of clouds and aerosols occurrence, structure and physical properties that are derived from measurements of solar and thermal radiation.
EarthCARE (Earth Clouds, Aerosols and Radiation Explorer) is one of the future earth observation mission of ESA and JAXA. The satellite will carry four instruments for observation of clouds and aerosols; Atmospheric Lidar (ATLID), Cloud Profiling Rader (CPR), Multi-Spectral Imager (MSI), and Broad-Band Radiometer (BBR). This mission aims at understanding of the role that clouds and aerosols play in reflecting incident solar radiation back into space and trapping infrared radiation emitted from Earth’s surface. These observations are needed to improve the precision of climate variability prediction.
MSI provides across-track information on cloud with channels in the visible, near infrared, shortwave and thermal infrared. Water cloud optical properties are derived in using EarthCARE/MSI standard product based on CLAUDIA [Ishida and Nakajima, 2009] and CAPCOM [Nakajima and Nakajima, 1995; Kawamoto et al., 2001]. Research product based on MWP method [M. Hashimoto, 2015. PhD Thesis] is advanced to obtain the ice cloud optical properties. In this presentation, development of the cloud analysis algorithms will be introduced.

Keywords: EarthCARE, cloud

Development of remote sensing algorithm to retrieve aerosol optical properties and introduction of the results of case studies

*Makiko Hashimoto[1], Hideaki Takenaka[1], Akiko Higurashi[2], Teruyuki Nakajima[1]

1.Japan Aerospace Explortion Agency, 2.NIES

We have developed a satellite remote sensing algorithm to retrieve the aerosol optical properties using multi-wavelength and multi-pixel information of satellite imagers (MWP). We simultaneously retrieve several parameters that characterize pixels, such as aerosol optical thickness (AOT) of fine and coarse mode particles, single scattering albedo (SSA), and ground surface albedo of each observed wavelength, in each of horizontal sub-domains consisting the target area.
We applied the algorithm to GOSAT/TANSO-CAI and Himawari-8/AHI data. We will show the retrieval results of aerosol characteristics over the urban and forest fire regions such as the Kanto area in Japan and Beijing in China. We also tried to retrieve aerosol properties at a forest fire case, so we would like to introduce the retrieval results over the forest fire regions in Indonesia.
From the results, AOT over the urban or high population areas is larger than that around rural or the low population areas. Furthermore, the SSA is lower in the urban region. For the forest fire case, the AOT and SSA along the plume are higher and lower than that of the other region, respectively. Although the AOT of fine mode totally looks dominant, the Angstrom exponent around the hot spot is lower than that of the leeward side, and increase with the increasing distance from the hot spot.

Keywords: Remote sensing, Aerosol, Satellite

Eddy Effect on the Kuroshio East of Taiwan from Satellite Altimetry

*Chungru Ho[1], Po-Chun Hsu[1], Chen-Chih Lin[1], Shih-Jen Huang[1]

1.Natl. Taiwan Ocean Univ.

Kuroshio is a western boundary current in the North Pacific Ocean. It flows northward along the east coast of Taiwan. Previous studies have shown that there is an eddy-rich zone located at 18°-26°N, 122°-160°E. The westward propagating eddies may affect the axis of Kuroshio when they impinge the Kuroshio east of Taiwan. To more understand the phenomenon, satellite altimeter data are used to investigate effects of oceanic mesoscale eddy on the Kuroshio from 18°N to 26°N. The Kuroshio axis is defined as a line with the maximum surface velocity along the Kuroshio path. The velocity of Kuroshio is calculated from the absolute dynamic topography data derived from satellite altimetry with the geostrophic relations. The results show that the Kuroshio meander occurred 13 times from 1993 to 2013 which were caused by westward or northward moving cold eddies when they propagated to the east of Taiwan. The average duration of the meanderings was 27 ±20 days, and the maximum duration was 80 days. The farthest position of the Kuroshio axis meandering was approximately 270 km from the average Kuroshio axis. It is affected by the size of the cold eddy. Under the circumstances of a cold eddy, the mean speed of the Kuroshio axis drops to 0.63 m/s, which is approximately 84% of the seasonal average.

Keywords: Kuroshio, meander, eddy, satellite altimetry

The Central-Pacific type of ENSO and its connection to Pacific Meridional Mode

*ChunYi Lin[1]

1.National Museum of Marine Science & Technology

In this study, we examine the simulation of the Pacific meridional mode in pre-industrial experiments of the Coupled Model Intercomparison Projects Phase (CMIP5) and link the Pacific meridional mode simulations to the simulation of the Central-Pacific (CP) and Eastern-Pacific (EP) types of El Niño Southern Oscillation (ENSO). Objective criteria are developed to evaluate the model performance in Pacific meridional mode simulations, which gauge the intensity, spatial pattern, air-sea coupling strength, and persistence strength of the coupling of the model meridional mode. Our analyses indicate that most of the CMIP5 model overestimate the air-sea coupling strength in the subtropical where the Pacific meridional mode model occurs, but underestimate the persistence of the coupling. Based on our criteria, ten CMIP5 models are found capable of realistically simulating the Pacific meridional mode. Further analyses reveal that CMIP5 model simulations of the CP ENSO is linked to the model performance in simulating the Pacific meridional mode; the models that are more capable of simulating the Pacific meridional mode also produce stronger CP ENSO. This study demonstrates that the subtropical dynamics and coupling affect the ability of CMIP5 models in simulating the different flavors of ENSO, which should be considered as one of the importance matrices for CMIP5 model evaluation.

Keywords: Central-Pacific types of ENSO, Eastern-Pacific types of ENSO, Pacific meridional mode

Validation of AMSR2 ocean products –Construction of validation system–

*Tsutomu Hihara[1], Hiroyuki Tomita[2]

1.Tokai University, Doctor's Course of Earth and Environmental Science, 2.Nagoya University, Institute for Space-Earth Environmental Research

In Global Change Observation Mission (GCOM), a satellite named GCOM-Water (GCOM-W) was launched in May 2012 to observe the effective geophysical parameters for understanding the global change of water cycle. The Japan Aerospace Exploration Agency (JAXA) has provided the ocean products (sea surface temperature and sea surface wind speed), which are made from brightness temperature observed by the Advanced Microwave Scanning Radiometer 2 (AMSR2) loaded onto GCOM-W, since May 2013. In general, satellite products are updated frequently, because the validation of data and the development of algorithm continue after these were released. The JAXA already updated the AMSR2 ocean products one time and will continue the updating. Accordingly, we tried to develop a validation system (VS) offering continuously and speedily the significant information for improvement of products in order to validate the AMSR2 ocean products from a long-term perspective and under a unified reference.

The VS mainly consists of two components. The first component is “Inter-comparison between the several gridded data”. In this component, the VS outputs the spatial distributions of average and standard deviation for each grid datum, the time series of the regional mean, and the mean difference and the Root Mean Square (RMS) difference between the grid data and the reference data that are made preparations in advance. The second component is “Comparison with in situ data”. In this component, the grid data are compared with high quality meteorological data observed by the moored buoys or the ships. As a result, the basic statistics (bias, RMS error, correlation coefficient and so on) and the figures (scatter plot and time series on buoy positions) are obtained. About the above-mentioned results, we can graphically check by the html files, which are automatically created in the VS.

As an example, we show the screenshots of results of comparison between AMSR2 sea surface temperature data and moored buoy data in an attached figure. In this result, AMSR2 data were validated using 24,660 daily mean data observed by 97 moored buoys from 2012 to 2014. We can check not only the results for all buoy data, but also the results for each year, each band of latitude, and each buoy.

Keywords: GCOM-W, AMSR2, mooring buoy data, marine meteorology, sea surface temperature

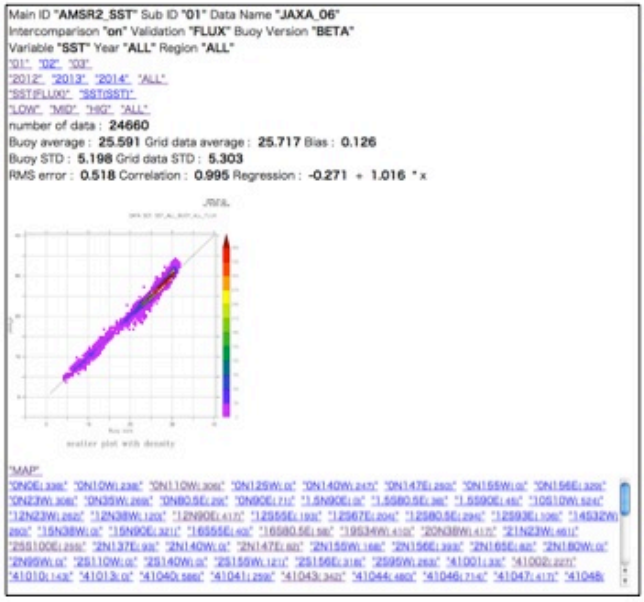

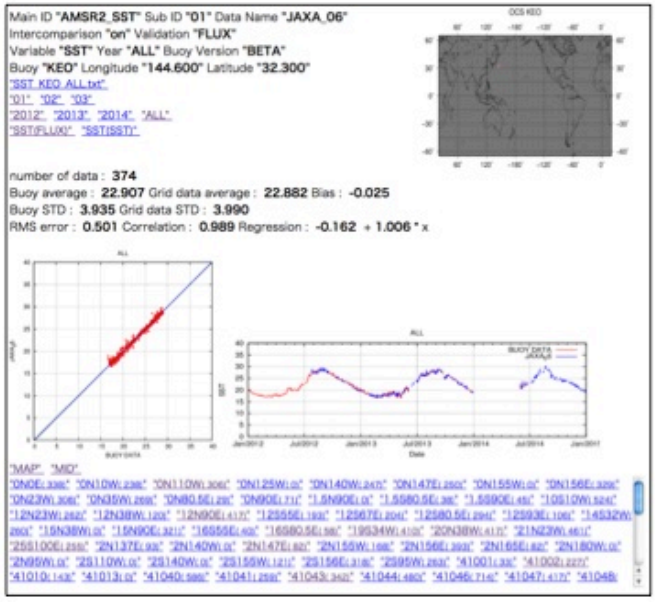

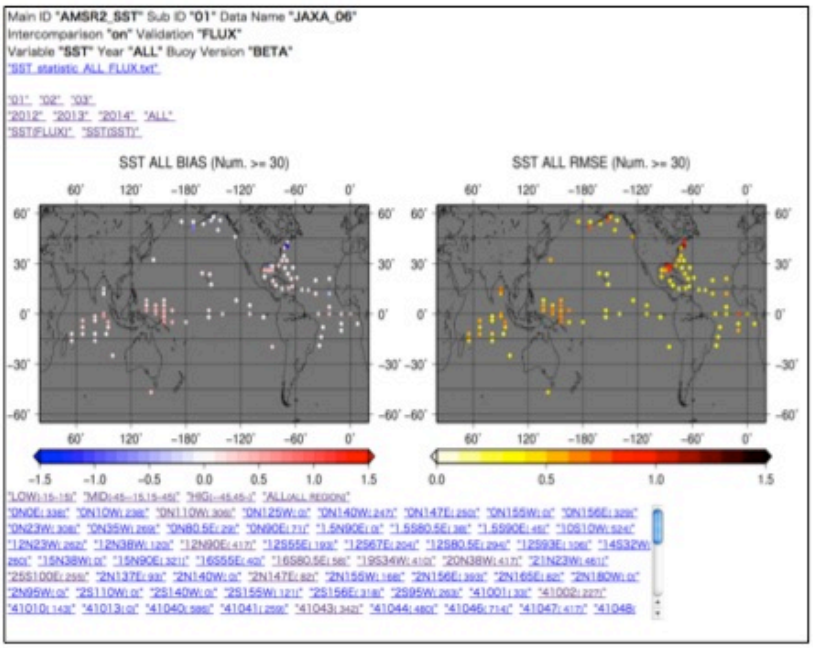

Applying Big Data Analysis Method to Improvement Sea Surface Temperature of Geostationary Satellite.

*Yung Shiang Lee[1], Feng Chun Su[2], Yu Mei Yeh[1], Chun Yi Lin[2], Yu Hsin Chen[3]

1.Department of Marketing & Distributioin Management, Hsiang Wu University, 2.National Museum of Marine Science & Technology , Taiwan, 3.State Key Laboratory of Marine Environmental Science, College of Ocean and Earth Sciences, Xiamen University, Xiamen, China

Big Data is the amount of data involved enormous and cannot be the information within a reasonable period of time to query, retrieve, manage, and analyze. The Big Data are three qualities: Volume, Velocity, and Variety, which information in many fields have brought progress and a breakthrough opportunity. Recent studies sea surface temperature mostly as a reference material Moderate Resolution Imaging Spectroradiometer (MODIS). Sun-synchronous satellites significantly better than geostationary satellites at a time resolution. The equatorial region of the tropical Pacific SST bias main factors are wind speed and air temperature in past studies. In this study, used big data commonly algorithms to provide sea surface temperature (SST) image hourly data. We apply and compare data mining techniques to improve the quality of GOES SST product. By a logistic regression approach, the GOES SST can be determined with an accuracy of 0.4°K and an improvement of the correction to 95%.

Keywords: Big Data, Sea Surface Temperature, Tropical Pacific

The Evolution of internal wave from mode-one to mode-two

*fengchun Su[1]

1.National Museum of Marine Science & Technology

Internal waves (IWs) are observed in the ocean all over the world. In the northern South China Sea, internal waves are frequently monitored between the Luzon Strait and Hainan Island by several satellites, such as optical or radar satellites. The wave crest can be as long as 200 km. It's amplitude is larger than 170 m. The huge amplitude maybe the largest than that ever observed in the world's oceans. The huge IW is usually observed in the deep sea area between the Luzon Strait and Hainan Island. Then a small mode-two wave was observed following a huge mode-one IW on the shelf near Dong-Sha Atoll. Due to the different wave speeds, mode-one and mode-two waves would separate into two waves after decomposition on the shelf. Thus we though the huge model-one IW in deep sea area could be deposited into more modes of IW on the shelf.
In this study, the objective is to observe the generation and evolution of mode-one IWs in the deep sea area, and then the mode-one IW deposit into more modes of IWs on the shelf break. The generation of mode-two waves on the shelf by disintegration of mode-one IWs in the deep ocean is proposed and analyzed based on the theory of modal-decomposition. In this study, some historical measurement data and satellite image are used to detect IWs. Then , the environmental condition is from a mooring near Dong-Sha Island. For comparison, the characteristics of mode-one and mode-two waves from environmental parameters have been estimated. For the test case, water depth increases to 450 m the mode-two wave energy is decreasing to 14%, while it is increasing to 25% when water depth decreases to 350 m. So, the mode-two waves can be generated under favorable condition, especially for multiple layer stratification in the shallow water on shelf.

Keywords: internal wave, south china sea, mode-two

